

# Gravitino DM and high reheating temperatures after LHC 7/8

JAN HEISIG

*Institute for Theoretical Particle Physics and Cosmology,  
RWTH Aachen University, Germany*

The presence of high reheating temperatures in the thermal history of the universe challenges supersymmetric scenarios owing to the gravitino problem. We revise a general  $R$ -parity conserving gravitino dark matter scenario with a stau as the next-to-lightest superparticle being particularly constrained by searches for heavy stable charged particles at the LHC. Imposing a variety of experimental and theoretical constraints we show that points with  $T_R > 10^9$  GeV survive only in a very particular corner of parameter space.

## 1 Introduction

An attractive way to explain the baryon asymmetry in the universe is thermal leptogenesis<sup>1</sup>. For this mechanism to work the universe has to be heated up to temperatures  $T_R \gtrsim 10^9$  GeV<sup>2,3</sup> in the post-inflationary phase of reheating. The recent observation of B-mode polarization of the CMB reported by the BICEP2 collaboration<sup>4</sup> could well be explained by GUT-scale inflation which in general is consistent with a reheating temperature in this ballpark.<sup>a</sup>

Once we want to accommodate such a high reheating temperature in the early universe supersymmetric scenarios potentially suffer from the gravitino problem<sup>5</sup>. Massive gravitinos are typically not in thermal equilibrium in the post-inflationary universe and the production due to thermal scattering in the hot bath renders their abundance proportional to the reheating temperature.<sup>6,7</sup> Hence, a high reheating temperature leads to a high gravitino abundance. In a scenario with a neutralino as the lightest superparticle (LSP) late decays of the gravitino cause an additional energy injection during or after big bang nucleosynthesis (BBN) distorting the predictions for the primordial abundances of light elements.<sup>8</sup> This imposes tight bounds on the maximal reheating temperature in this scenario and rules out thermal leptogenesis for a neutralino LSP and a gravitino mass of the order of the other sparticle masses.

One way to alleviate this problem is considering a gravitino LSP<sup>9</sup>. In this case the reheating temperature is only constrained via the measured dark matter (DM) abundance. However, now the next-to-LSP (NLSP) can only decay into the gravitino via Planck-suppressed couplings (we assume  $R$ -parity conservation here) leading to a rather large NLSP life-time. In this case late NLSP decays can endanger successful BBN and further constrain the model. However, if the NLSP belongs to the MSSM it interacts at least weakly and so the NLSP abundance is determined from freeze-out. Hence, it is the MSSM parameters that govern the consistency with BBN constraints and not the reheating temperature. Further, the gravitino abundance shows a non-trivial dependence on the MSSM parameters through thermal and non-thermal contributions. As the MSSM parameters can in principle be measured—or so far at least be constrained—by LHC data it is natural to ask whether these measurements provide implications for the highest reheating temperatures that are still consistent with observations.

---

<sup>a</sup>As an example, assuming an inflaton mass of the order of  $m_\phi \sim 10^{13}$  GeV (which fits the BICEP2 data in a simple chaotic inflation model with a quadratic potential) and that the inflaton decays dominantly via Planck-suppressed dimension-five operators,  $\Gamma_\phi \sim m_\phi^3/M_{\text{Pl}}^2$ , we obtain a reheating temperature in the ballpark of  $T_R \sim \sqrt{\Gamma_\phi M_{\text{Pl}}} \sim 10^9 \dots 10^{10}$  GeV.

In this article we summarize our research<sup>10,11</sup> which addresses this question considering the case of a stau NLSP. As in such a scenario the stau is stable on collider time-scales it provides a spectacular signature as a heavy stable charged particle (HSCP). The LHC is extremely sensitive to such a signal and thus wide implications can be derived. Other NLSP candidates are in general less constrained by the data.

In order to explore the SUSY parameter space we utilize a Monte Carlo scan which we briefly summarize in section 2. In section 3 we introduce the relevant mechanisms of gravitino production. We present our results in section 4. Our study reveals the existence of parameter points that provide  $T_R > 10^9$  GeV and survive all imposed constraints. All these points lie in a very particular corner of the SUSY parameter space. Those spectra feature a distinct signature at colliders that can be tested in the upcoming LHC run.

## 2 Monte Carlo scan

In order to explore the implications of the LHC and the results of other experiments on the highest reheating temperature we utilize a Monte Carlo scan over the SUSY parameter space.<sup>11</sup> We do not restrict ourselves to any high scale model but vary the parameters freely at the TeV scale. We scanned over the 17-dimensional pMSSM parameter space with the following input parameters and scan ranges:

$$\begin{aligned}
-10^4 \text{ GeV} &\leq A_t &&\leq 10^4 \text{ GeV} \\
-8000 \text{ GeV} &\leq A_b, A_\tau, \mu &&\leq 8000 \text{ GeV} \\
1 &\leq \tan \beta &&\leq 60 \\
100 \text{ GeV} &\leq m_A &&\leq 4000 \text{ GeV} \\
200 \text{ GeV} &\leq m_{\tilde{\tau}_1} &&\leq 2000 \text{ GeV} \\
\max(m_{\tilde{\tau}_1}, 700 \text{ GeV}) &\leq m_{\tilde{t}_1}, m_{\tilde{b}_1} &&\leq 5000 \text{ GeV} \\
0 &< \theta_{\tilde{\tau}}, \theta_{\tilde{t}} &&< \pi \\
m_{\tilde{\tau}_1} &\leq m_{\tilde{L}_{1,2}}, m_{\tilde{e}_{1,2}} &&\leq 4000 \text{ GeV} \\
\max(m_{\tilde{\tau}_1}, 1200 \text{ GeV}) &\leq m_{\tilde{Q}_{1,2}} = m_{\tilde{u}_{1,2}} = m_{\tilde{d}_{1,2}} &&\leq 8000 \text{ GeV} \\
m_{\tilde{\tau}_1} &\leq M_1, M_2 &&\leq 4000 \text{ GeV} \\
\max(m_{\tilde{\tau}_1}, 1000 \text{ GeV}) &\leq M_3 &&\leq 5000 \text{ GeV}
\end{aligned} \tag{1}$$

The lighter stau was taken to be the NLSP and we required that at least one of the neutral  $CP$ -even Higgses,  $m_h, m_H$ , can be identified with the Higgs boson discovered at the LHC<sup>12,13</sup>:  $m_h$  or/and  $m_H \in [123; 128]$  GeV. We generated  $10^6$  points obeying these requirements. For each point the stau freeze-out abundance<sup>14</sup> and a variety of observables were computed in order to apply experimental and theoretical bounds. Limits on the sparticle mass spectrum were derived from a reinterpretation<sup>11</sup> of the HSCP searches at the 7 and 8 TeV LHC by CMS<sup>15</sup>. Further, we considered bounds from flavor<sup>16,17</sup> and precision<sup>18,19</sup> observables, collider searches for the MSSM Higgs sector<sup>20</sup> as well as theoretical constraints from charge or color breaking (CCB) minima<sup>11,21</sup>.

For each point of the 17-dimensional pMSSM ten gravitino masses,  $m_{\tilde{G}}$ , were randomly chosen.<sup>10</sup> The gravitino mass range was determined from the minimum stau life-time  $\tau_{\tilde{\tau}_1} > 10^4$  sec (for the lower edge) and from an upper bound on the stau life-time arising from searches for anomalously heavy hydrogen in deep sea water (for the upper edge).<sup>10</sup> For the application of BBN bounds<sup>22,23</sup> and bounds from diffuse gamma ray observations<sup>24</sup> we computed the life-time and the hadronic branching ratios of the stau for each point.

### 3 Production of gravitinos

On the one hand, gravitinos are produced thermally during reheating. The corresponding relic abundance reads<sup>7</sup>

$$\Omega_{\tilde{G}}^{\text{th}} h^2 \simeq \sum_{i=1}^3 c_i g_i^2(T_{\text{R}}) \left( 1 + \frac{M_i^2(T_{\text{R}})}{3m_{\tilde{G}}^2} \right) \left( \frac{m_{\tilde{G}}}{100 \text{ GeV}} \right) \left( \frac{T_{\text{R}}}{10^{10} \text{ GeV}} \right), \quad (2)$$

where  $g_i$  and  $M_i$  are the gauge couplings and the gaugino mass parameters, respectively, associated with the SM gauge groups  $U(1)_Y$ ,  $SU(2)_L$ ,  $SU(3)_c$  and  $c_i$  are associated numerical factors of  $\mathcal{O}(0.1)$ . On the other hand, gravitinos are produced non-thermally from the decay of the NLSP after NLSP freeze-out. Due to the assumed  $R$ -parity conservation each stau eventually decays into a gravitino. Hence, the number density of staus before their decay,  $n_{\tilde{\tau}_1}$ , is equal to the number density of gravitinos after all staus have decayed,  $n_{\tilde{G}}$ , and thus

$$\Omega_{\tilde{G}}^{\text{non-th}} h^2 = \frac{m_{\tilde{G}}}{m_{\tilde{\tau}_1}} \Omega_{\tilde{\tau}_1} h^2 \simeq 3.7 \times 10^{-9} m_{\tilde{G}} Y, \quad (3)$$

where we introduced the stau yield,  $Y = n_{\tilde{\tau}_1}/s$ , with  $s$  being the entropy density. By demanding that the resulting total gravitino abundance matches the measured DM abundance,  $\Omega_{\tilde{G}}^{\text{non-th}} h^2 + \Omega_{\tilde{G}}^{\text{th}} h^2 = \Omega_{\text{CDM}} h^2$ , we computed the required abundance of thermally produced gravitinos,  $\Omega_{\tilde{G}}^{\text{th}} h^2$ . For  $\Omega_{\text{CDM}} h^2$ , we chose the best-fit value  $\Omega_{\text{CDM}} h^2 = 0.11889^{25}$ . From (2) we computed the reheating temperature,  $T_{\text{R}}$ , that provides  $\Omega_{\tilde{G}}^{\text{th}} h^2$  for the given parameter point.

### 4 Results and discussion

Figure 1 shows the ratio between the non-thermal and the thermal production of gravitinos. For small  $m_{\tilde{G}}$  the non-thermal contribution is unimportant and the resulting reheating temperature grows linearly with the gravitino mass. Once the gravitino mass approaches the mass of the other superpartners we encounter two effects. First, according to (2), the linear growth of  $T_{\text{R}}$  with  $m_{\tilde{G}}$  turns into a decrease when approaching small mass splittings between the gravitino and the gaugino masses. This effect causes the points with the highest  $T_{\text{R}}$  to lie around gravitino masses of a few hundred GeV. This number is a consequence of the chosen mass ranges for the gaugino mass parameters in our scan. The absolute maximum of  $T_{\text{R}}$  reached in our scan depends upon the lower limits of the scan ranges for the gaugino masses which are 200 GeV for  $M_1$ ,  $M_2$  and 1 TeV for  $M_3$ . It reaches  $T_{\text{R}} \simeq 4 \times 10^9$  GeV in accordance with conservative limits found earlier<sup>26</sup>. As a second effect, once the gravitino mass approaches the mass of the stau NLSP, non-thermal contributions become important. Depending on the stau yield of a considered point the required reheating temperature is pushed down by a more or less significant amount. The points that still stay close to the upper edge of the populated band when  $m_{\tilde{G}}$  approaches  $m_{\tilde{\tau}_1}$  tend to be those with very small yields. However, we found points with yields  $Y \gtrsim 10^{-13}$  for  $T_{\text{R}} \gtrsim 10^9$  GeV. For these points the non-thermal contribution to the gravitino production is of the same order of magnitude as the thermal contribution and cannot be neglected.

Figure 2 shows the effect of the bounds imposed on the  $(17 + 1)$ -dimensional parameter space. The blue points are rejected by the direct SUSY searches (i.e., the searches for HSCP). The yellow points are rejected by additional bounds from flavor and precision observables, MSSM Higgs searches or CCB bounds. The red points are rejected by the BBN bounds or the bounds from the diffuse gamma ray spectrum. The green points satisfy all constraints. The searches for HSCP at the 7 and 8 TeV LHC impose very restrictive limits on the gluino and wino masses.<sup>11,27</sup>

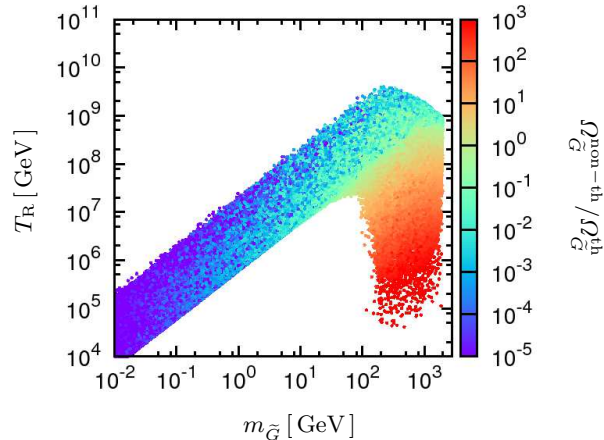


Figure 1: Points of the  $(17 + 1)$ -dimensional pMSSM scan in the  $m_{\tilde{G}}-T_R$  plane. Color code: Ratio between the non-thermal and thermal contribution to the gravitino abundance,  $\Omega_{\tilde{G}}^{\text{non-th}}/\Omega_{\tilde{G}}^{\text{th}}$ .

In our scan we do not find allowed points with  $m_{\tilde{g}} < 1.2 \text{ TeV}$  or  $M_2 < 800 \text{ GeV}^b$  (see lower panels of figure 2). Hence, these searches exclude all points with a reheating temperature above  $T_R \simeq 2.3 \times 10^9 \text{ GeV}$  (cf. blue versus yellow points). The very strong and robust limits on the SUSY masses are a particular feature of the stau NLSP scenario.<sup>11,27</sup> For other choices of the NLSP these bounds can be considerably weaker, potentially leaving more room for  $T_R \gtrsim 10^9 \text{ GeV}$ . Note that the bound on  $M_2$  is particularly important. The gaugino masses in (2) have to be evaluated at the scale  $T_R$ . Due to the faster running of  $M_2$  with respect to  $M_3$  up to  $T_R$  the  $SU(2)_L$  contribution can easily become dominant despite the smaller coupling. Bounds from flavor and precision observables, MSSM Higgs searches and CCB vacua further reduce the parameter space leaving a maximal reheating temperature of slightly below  $2 \times 10^9 \text{ GeV}$  (cf. yellow versus red points) in our scan. The application of BBN bounds has the most significant effect in the region of large  $\Omega_{\tilde{G}}^{\text{non-th}}/\Omega_{\tilde{G}}^{\text{th}}$  where  $Y$  and  $m_{\tilde{G}}$  (and therefore  $\tau_{\tilde{\tau}_1}$ ) are large.

Despite the restrictive limits from HSCP searches in this scenario we find points which provide reheating temperatures  $T_R > 10^9 \text{ GeV}$  and are consistent with all discussed bounds and with a Higgs mass of around  $125 \text{ GeV}$ . All these points share very distinct features. First, these points feature gaugino masses not far above their respective lower limits imposed by HSCP searches and a relatively heavy gravitino,  $300 \text{ GeV} < m_{\tilde{G}} < 1.4 \text{ TeV}$ , in order to minimize (2). Second, BBN bounds and bounds from the diffuse gamma ray spectrum disfavor very large lifetimes and do not allow for  $\tau_{\tilde{\tau}_1} > 10^7 \text{ sec}$  in our scan (see upper right panel of figure 2). Hence, we encounter a separation between the gravitino mass and the stau mass of at least  $200 \text{ GeV}$ . This separation coincides with the one between the gravitino mass and the gaugino masses in such a way that we find rather small mass splittings between the stau and the gauginos. This is most pronounced for  $M_2$ . As a consequence the strong bounds on  $m_{\tilde{g}}$  and  $M_2$  also lift up the stau masses for points with  $T_R > 10^9 \text{ GeV}$  in our scan, which we found to lie above  $m_{\tilde{\tau}_1} \simeq 800 \text{ GeV}$ . Third, from BBN bounds those points are required to feature exceptionally small yields  $Y < 3 \times 10^{-14}$  being allowed only in region of parameter space where annihilation dominantly occurs via a resonant heavy Higgs in the  $s$ -channel,  $m_A \simeq 2m_{\tilde{\tau}_1}$ .<sup>11</sup> For most points the dominant annihilation process is resonant stau-pair annihilation<sup>28</sup>. However, we also found a few points where resonant stop or EWino co-annihilation<sup>11</sup> is the dominant process. Note that EWino co-annihilation via a resonant heavy Higgs requires no particularly large Higgs-sfermion couplings. Thus, the viability of these points does not rely on constraints from CCB vacua. As

<sup>b</sup>These limits can be understood as conservative limits on the individual parameters. Since we combine production channels for the derivation of exclusion limits in our scan, in general points with masses above these limits can be excluded.

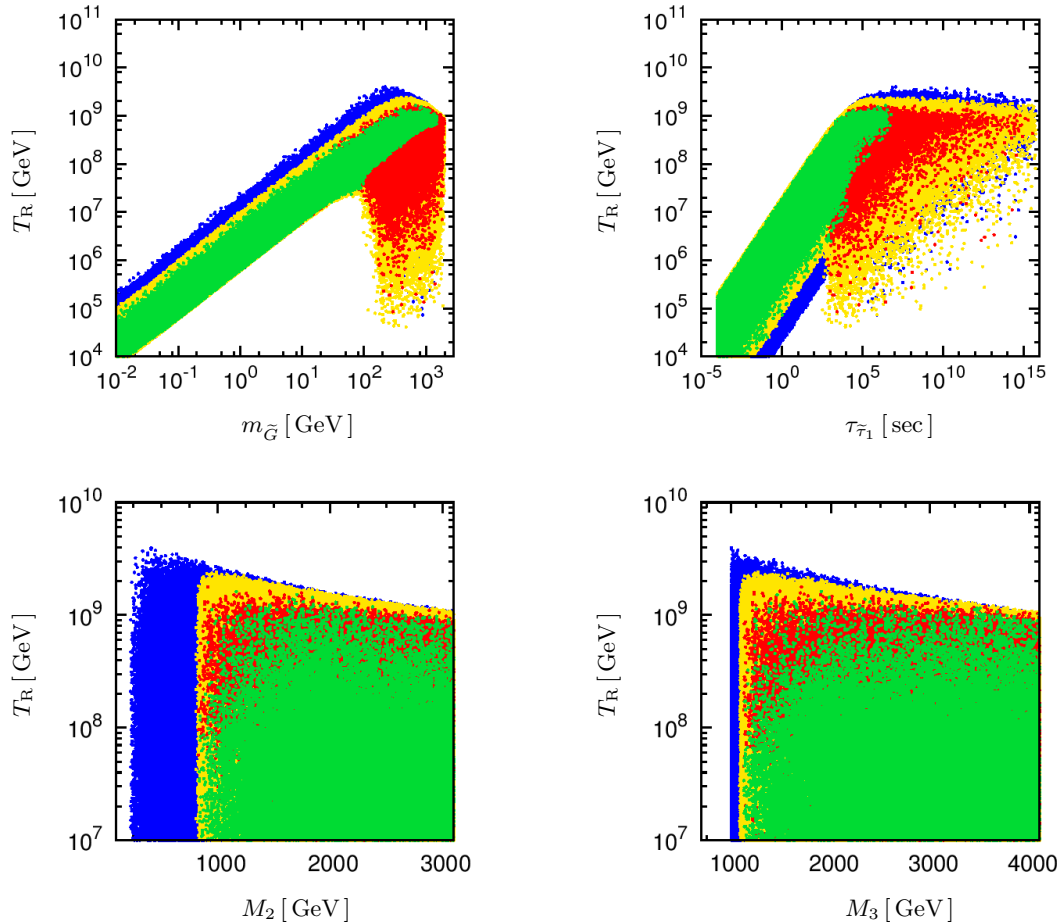


Figure 2: Points of the  $(17 + 1)$ -dimensional pMSSM scan. The color code is chosen as follows. Blue: Points passing no constraints. Yellow: Points passing constraints from the HSCP search. Red: Points additionally passing the constraints from flavor and precision observables, MSSM Higgs searches and CCB bounds. Green: Points additionally passing the BBN bounds and bounds from the diffuse gamma ray spectrum. Upper left panel: Reheating temperature  $T_R$  against the gravitino mass  $m_{\tilde{G}}$ . Upper right panel: Reheating temperature  $T_R$  against the stau life-time  $\tau_{\tilde{\tau}_1}$ . Lower left panel: Reheating temperature  $T_R$  against the wino mass parameter  $M_2$ . Lower right panel: Reheating temperature  $T_R$  against the gluino mass parameter  $M_3$ .

in this case the annihilation is driven by pair-annihilating EWinos it shows that similarly small yields could as well be achieved in a neutralino NLSP scenario.

## 5 Conclusion

In this article we examined the interplay between constraints on the SUSY parameter space and the highest possible reheating temperatures in a gravitino-stau scenario taking into account the thermal and non-thermal production of gravitinos. We found valid points with a reheating temperature high enough to allow for thermal leptogenesis,  $T_R \gtrsim 10^9$  GeV. These points are consistent with BBN bounds, flavor and precision bounds, theoretical bounds from vacuum stability, bounds from the HSCP searches at the 7 and 8 TeV LHC as well as bounds from the MSSM Higgs searches and the requirement of providing a Higgs around 125 GeV. In order to pass the BBN bounds all these points feature exceptionally small stau yields,  $Y \lesssim 10^{-14}$ , that are only allowed in the resonant region,  $m_A \simeq 2m_{\tilde{\tau}_1}$ . In this region annihilation dominantly takes place via the exchange of an  $s$ -channel heavy Higgs either via resonant stau pair annihilation or resonant co-annihilating sparticles.

For most of the points with  $T_R > 10^9$  GeV the dominant production mode at the 13/14 TeV LHC would be the production of EWinos or gluinos being relatively close in mass to the stau. Further, due to the resonant configuration,  $m_A \simeq 2m_{\tilde{\tau}_1}$ , resonant stau production via the s-channel heavy Higgs would be an important contribution. At the 13/14 TeV LHC this open window for high reheating temperatures can be tested.

The gaugino masses  $M_2$  and  $M_3$  are of particular importance here. For other NLSP candidates the respective mass limits can be much weaker than in the present case of a stau NLSP. For  $M_2$  and  $M_3$  close to the lower edges of our scan ranges,  $M_2 \gtrsim 200$  GeV and  $M_3 \gtrsim 1$  TeV we found a maximum reheating temperature of around  $T_R \simeq 4 \times 10^9$  GeV. Provided an equally efficient annihilation of the NLSP candidate and similar constraints from BBN we expect temperatures around this value to be maximally allowed in a neutralino NLSP scenario.

## Acknowledgements

I would like to thank Jörn Kersten, Boris Panes and Tania Robens for a fruitful collaboration and Valerie Domcke and Marco Drewes for very helpful discussions. Further, I wish to thank the Moriond organizers for financial support. This work was partly supported by the German Research Foundation (DFG) via the Junior Research Group ‘SUSY Phenomenology’ within the Collaborative Research Center 676 ‘Particles, Strings and the Early Universe’.

## References

1. M. Fukugita and T. Yanagida, *Phys. Lett.* **B174** (1986) 45.
2. S. Davidson and A. Ibarra, *Phys.Lett.* **B535** (2002) 25–32.
3. W. Buchmüller, P. Di Bari, and M. Plumacher, *Annals Phys.* **315** (2005) 305–351.
4. BICEP2 Collaboration, P. Ade *et al.*, [arXiv:1403.3985 \[astro-ph.CO\]](#).
5. S. Weinberg, *Phys. Rev. Lett.* **48** (1982) 1303.
6. M. Bolz, A. Brandenburg, and W. Buchmüller, *Nucl. Phys.* **B606** (2001) 518–544.
7. J. Pradler and F. D. Steffen, *Phys. Lett.* **B648** (2007) 224–235.
8. J. R. Ellis, D. V. Nanopoulos, and S. Sarkar, *Nucl. Phys.* **B259** (1985) 175.
9. P. Fayet, in *Proceedings of the XVIIth Rencontre de Moriond*, pp. 347–367, 1981.
10. J. Heisig, *JCAP* **04** (2014) 023.
11. J. Heisig, J. Kersten, B. Panes, and T. Robens, *JHEP* **04** (2014) 053.
12. ATLAS Collaboration, ATLAS-CONF-2013-014, 2013.
13. CMS Collaboration, CMS-PAS-HIG-13-005, 2013.
14. G. Belanger *et al.*, *Comput. Phys. Commun.* **180** (2009) 747–767.
15. CMS Collaboration, S. Chatrchyan *et al.*, *JHEP* **1307** (2013) 122.
16. Heavy Flavor Averaging Group, Y. Amhis *et al.*, 2012.
17. LHCb Collaboration, R. Aaij *et al.*, *Phys. Rev. Lett.* **110** (2013) 021801.
18. Tevatron Electroweak Working Group, [arXiv:1204.0042 \[hep-ex\]](#).
19. P. Bechtle *et al.*, *Eur. Phys. J.* **C73** (2013) 2354.
20. P. Bechtle *et al.*, *Comput. Phys. Commun.* **182** (2011) 2605–2631.
21. T. Kitahara and T. Yoshinaga, *JHEP* **1305** (2013) 035.
22. K. Jedamzik, *JCAP* **0803** (2008) 008.
23. K. Jedamzik, *Phys. Rev.* **D74** (2006) 103509.
24. G. D. Kribs and I. Z. Rothstein, *Phys. Rev.* **D55** (1997) 4435–4449.
25. Planck Collaboration, P. A. R. Ade *et al.*, [arXiv:1303.5076 \[astro-ph.CO\]](#).
26. M. Endo, K. Hamaguchi, and K. Nakaji, [arXiv:1105.3823 \[hep-ph\]](#).
27. J. Heisig and J. Kersten, *Phys. Rev.* **D86** (2012) 055020.
28. J. Pradler and F. D. Steffen, *Nucl. Phys.* **B809** (2009) 318–346.